

Investigating Auto-correlation of Scattered Light of Mixed Particles

Yong Sun*

July 7, 2018

Abstract

In this work, the normalized time auto-correlation function of the electric field of the light $g^{(1)}(\tau)$ that is scattered by the two kinds of particles in dispersion is investigated. The results show that the logarithm of $g^{(1)}(\tau)$ can be consistent with a line and many reasons can cause the deviations between an exponentiality and plots of $g^{(1)}(\tau)$ as a function of delay time τ . The nonexponentiality of $g^{(1)}(\tau)$ is not only determined by the particle size distribution and scattering angle but also greatly influenced by the relationship between the concentrations, mass densities and the values that the refractive index of the material expands as a function of the concentration of the two kinds of particles.

1 INTRODUCTION

For colloidal dispersion systems, light scattering is a widely used technique to measure the sizes of particles. The dynamic light scattering (DLS) technique is to measure the particle sizes from the normalized time auto-correlation function of the scattered light $g^{(2)}(\tau)$. The cumulants [1–4] has been used as a standard method to obtain the polydispersity of particles from the DLS data. In general, when the DLS data are analyzed, the size distribution of particles is considered as a mono-disperse distribution if the logarithm of the normalized time auto-correlation function of the electric field of the light $g^{(1)}(\tau)$ is consistent with a line. The poly-dispersity of the particles is obtained from the deviation between an exponentiality and $g^{(1)}(\tau)$.

In the previous work [5, 6], for the particles that the number distribution is Gaussian, it has been discussed that the nonexponentiality of $g^{(2)}(\tau)$ is determined by the particle size distribution and scattering angle. In general, the effects of the particle size distribution are small on the deviation between an exponentiality and $g^{(2)}(\tau)$ and very large on the initial slope of the logarithm of $g^{(2)}(\tau)$ and the effects of the scattering angle are determined by the particle size distribution and mean particle size. Under some conditions, the nonexponentiality of $g^{(2)}(\tau)$ is greatly influenced by the scattering angle.

*Email: ysun2002h@yahoo.com.cn

In this work, the normalized time auto-correlation function of the electric field of the light $g^{(1)}(\tau)$ that is scattered by two kinds of particles in dispersion is investigated. The results show that the logarithm of $g^{(1)}(\tau)$ can be consistent with a line and many reasons can cause the deviations between an exponentiality and plots of $g^{(1)}(\tau)$ as a function of delay time τ . The nonexponentiality of $g^{(1)}(\tau)$ is not only determined by the particle size distribution and scattering angle but also greatly influenced by the relationship between the concentrations, mass densities and the values that the refractive index of the material expands as a function of the concentration of the two kinds of particles in dispersion.

2 THEORY

For the two kinds of dilute poly-disperse homogeneous spherical particles in dispersion where the Rayleigh-Gans-Debye approximation is valid, the total normalized time auto-correlation function of the electric field of the scattered light $g^{(1)}(\tau)$ can be written as

$$g_{total}^{(1)}(\tau) = \frac{g_1^{(1)}(\tau) + \frac{I_{s2}}{I_{s1}} g_2^{(1)}(\tau)}{1 + \frac{I_{s2}}{I_{s1}}}, \quad (1)$$

where I_{s1} , I_{s2} , $g_1^{(1)}(\tau)$ and $g_2^{(1)}(\tau)$ can be obtained as [7]

$$\frac{I_{s1}}{I_{inc}} = \frac{4\pi^2 \sin^2 \vartheta n_s^2 \left(\frac{dn_1}{dc_1} \right)_{c_1=0}^2}{\lambda^4 r^2} \frac{c_1}{3} \frac{4\pi \rho_1 \int_0^\infty R_{s1}^6 P(q, R_{s1}) G(R_{s1}) dR_{s1}}{\int_0^\infty R_{s1}^3 G(R_{s1}) dR_{s1}}, \quad (2)$$

$$\frac{I_{s2}}{I_{inc}} = \frac{4\pi^2 \sin^2 \vartheta n_s^2 \left(\frac{dn_2}{dc_2} \right)_{c_2=0}^2}{\lambda^4 r^2} \frac{c_2}{3} \frac{4\pi \rho_2 \int_0^\infty R_{s2}^6 P(q, R_{s2}) G(R_{s2}) dR_{s2}}{\int_0^\infty R_{s2}^3 G(R_{s2}) dR_{s2}}, \quad (3)$$

$$g_1^{(1)}(\tau) = \frac{\int R_{s1}^6 P(q, R_{s1}) G(R_{s1}) \exp(-q^2 D_1 \tau) dR_{s1}}{\int R_{s1}^6 P(q, R_{s1}) G(R_{s1}) dR_{s1}}, \quad (4)$$

$$g_2^{(1)}(\tau) = \frac{\int R_{s2}^6 P(q, R_{s2}) G(R_{s2}) \exp(-q^2 D_2 \tau) dR_{s2}}{\int R_{s2}^6 P(q, R_{s2}) G(R_{s2}) dR_{s2}}, \quad (5)$$

here ϑ is the angle between the polarization of the incident electric field and the propagation direction of the scattered field, c is the mass concentration of particles, r is the distance between the scattering particle and the point of the intensity measurement, ρ is the density of the particles, I_{inc} is the incident light intensity, I_s is the intensity of the scattered light that reaches the detector, R_s is the static radius of a particle, $q = \frac{4\pi}{\lambda} n_s \sin \frac{\theta}{2}$ is the scattering vector, λ is the wavelength of the incident light in vacuo, n_s is the solvent refractive index, θ is the scattering angle, $P(q, R_s)$ is the form factor of homogeneous spherical particles

$$P(q, R_s) = \frac{9}{q^6 R_s^6} (\sin(qR_s) - qR_s \cos(qR_s))^2 \quad (6)$$

and $G(R_s)$ is the number distribution of particle sizes. In this work, the number distribution is chosen as a Gaussian distribution

$$G(R_s; \langle R_s \rangle, \sigma) = \frac{1}{\sigma\sqrt{2\pi}} \exp\left(-\frac{1}{2}\left(\frac{R_s - \langle R_s \rangle}{\sigma}\right)^2\right), \quad (7)$$

where $\langle R_s \rangle$ is the mean static radius and σ is the standard deviation, From the Einstein-Stokes relation, the diffusion D can be written as

$$D = \frac{k_B T}{6\pi\eta_0 R_h}, \quad (8)$$

where η_0 , k_B , T and R_h are the viscosity of the solvent, Boltzmann's constant, absolute temperature and hydrodynamic radius, respectively. The subscripts 1 and 2 show the kinds of the particles in dispersion.

When $q \rightarrow 0$, the Z-average diffusion coefficient $\langle D \rangle_z$ can be written as

$$\langle D \rangle_z = \frac{\frac{\int_0^\infty R_{s1}^6 G(R_{s1}) D_1 dR_{s1}}{\int_0^\infty R_{s1}^6 G(R_{s1}) dR_{s1}} + a \frac{\frac{\int_0^\infty R_{s2}^6 G(R_{s2}) dR_{s2}}{\int_0^\infty R_{s2}^3 G(R_{s2}) dR_{s2}} \frac{\int_0^\infty R_{s2}^6 G(R_{s2}) D_2 dR_{s2}}{\int_0^\infty R_{s2}^6 G(R_{s2}) dR_{s2}}}{\frac{\int_0^\infty R_{s1}^6 G(R_{s1}) dR_{s1}}{\int_0^\infty R_{s1}^3 G(R_{s1}) dR_{s1}}}}{1 + a \frac{\frac{\int_0^\infty R_{s2}^6 G(R_{s2}) dR_{s2}}{\int_0^\infty R_{s2}^3 G(R_{s2}) dR_{s2}}}{\frac{\int_0^\infty R_{s1}^6 G(R_{s1}) dR_{s1}}{\int_0^\infty R_{s1}^3 G(R_{s1}) dR_{s1}}}} \quad (9)$$

where $a = \frac{\left(\frac{dn_2}{dc_2}\right)_{c_2=0}^2 c_2 \rho_2}{\left(\frac{dn_1}{dc_1}\right)_{c_1=0}^2 c_1 \rho_1}$

3 RESULTS AND DISCUSSION

In the previous work [7, 8], it was shown that the expected values of the DLS data calculated based on the commercial and static particle size information are consistent with the experimental data. In order to investigate the effects of the mixture of two kinds of particles on the deviation between an exponentiality and $g^{(1)}(\tau)$ accurately, the values of $g^{(1)}(\tau)$ were produced directly using Eqs. 1, 4 and 5, respectively.

The values of $g_1^{(1)}(\tau)$, $g_2^{(1)}(\tau)$ and $g_{total}^{(1)}(\tau)$ were produced using the information: the temperature T , viscosity of the solvent η_0 , wavelength of laser light λ , refractive index of the water n_s and constant R_h/R_s were set to 300.49K, 0.8479 mPa·S, 632.8 nm, 1.332 and 1.1, scattering angle θ was chosen as 30° and 90°, mean static radius $\langle R_s \rangle$ was set to 20 nm, 40 nm, 120 nm and 200 nm and standard deviation σ was 5% or 20% of the mean static radius, respectively.

First investigating the simple situation that the two kinds of particles have same c , ρ and $\left(\frac{dn}{dc}\right)_{c=0}$ or $a = 1$. The values of $\ln\left(g_1^{(1)}(\tau)\right)$, $\ln\left(g_2^{(1)}(\tau)\right)$ and $\ln\left(g_{total}^{(1)}(\tau)\right)$ produced using $\langle R_s \rangle$ and σ 20 nm, 1 nm and 40 nm, 2 nm are shown in Figs. 1a and 1b for scattering angles 30° and 90°, respectively. Both the results show that the plots of $\ln\left(g_{total}^{(1)}(\tau)\right)$ as a function of delay time τ are consistent with a line respectively and the mixture of the two kinds of particles with the narrow size distributions investigated

do not causes the nonexponentiality of $g_{total}^{(1)}(\tau)$ at the scattering angles investigated. Figure 1 also reveals that the values of $g_{total}^{(1)}(\tau)$ almost are determined by the kind of particles with the larger mean static radius. It agrees with the fact that most of scattered light comes from the kind of particles with the larger mean static radius under the condition $a = 1$.

In general, the values of concentration c , mass density ρ and the refractive index of the material expands as a function of the concentration $(\frac{dn}{dc})_{c=0}$ are different when the two kinds of particles are mixed. The values of $\ln(g_{total}^{(1)}(\tau))$ thus were calculated under the conditions $a = 5, 10$, respectively. In order to investigate the effects of a on $\ln(g_{total}^{(1)}(\tau))$, the results for $a = 1, 5$ and 10 are shown in Figs. 2a and 2b for scattering angles 30° and 90° , respectively. The results reveal that the larger the value of a , the larger the deviations between a line and plots of $\ln(g_{total}^{(1)}(\tau))$ as a function of delay time τ . Comparing to Fig. 1, the values of $\ln(g_{total}^{(1)}(\tau))$ obviously affected by the relative scattered light intensity or c, ρ and $(\frac{dn}{dc})_{c=0}$ of the two kinds of particles in dispersion.

For wide particle size distributions, the effects of the mixture of two kinds of particles on the plots of $\ln(g_{total}^{(1)}(\tau))$ as a function of delay time τ are investigated continually. The values of $\ln(g_1^{(1)}(\tau))$, $\ln(g_2^{(1)}(\tau))$ and $\ln(g_{total}^{(1)}(\tau))$ were produced using $\langle R_s \rangle$ and σ 20 nm, 4 nm and 40 nm, 8 nm, respectively. As exploring the narrow particle size distributions, the simple situation $a = 1$ is investigated first. All results are shown in Figs. 3a and 3b for scattering angles 30° and 90° , respectively. Figure 3 shows that the plots of $\ln(g_{total}^{(1)}(\tau))$ as a function of delay time τ are deviated from a line and the values almost are determined by the kind of particles with the larger mean static radius. Comparing to the plots of $\ln(g_1^{(1)}(\tau))$ and $\ln(g_2^{(1)}(\tau))$, the nonexponentiality of $g_{total}^{(1)}(\tau)$ is large.

Figure 3 shows the same results as Fig. 1 that the values of $g_{total}^{(1)}(\tau)$ almost are determined by the kind of particles with the larger mean static radius. In order to investigate the general situation that the two kinds of particles are mixed, the values of $\ln(g_{total}^{(1)}(\tau))$ were calculated under the conditions $a = 5, 10$, respectively. The results for $a = 1, 5$ and 10 are shown in Figs. 4a and 4b for scattering angles 30° and 90° , respectively. The results reveal the same situation as the particles with narrow particle size distribution that the larger the value of a , the larger the deviations between a line and plots of $\ln(g_{total}^{(1)}(\tau))$ as a function of delay time τ . Comparing to Fig. 3, the values of $\ln(g_{total}^{(1)}(\tau))$ obviously affected by the relative scattered light intensity or c, ρ and $(\frac{dn}{dc})_{c=0}$ of the two kinds of particles.

When the mean static radius is large enough, it is possible that the scattered intensity of the kind of particles with the smaller mean static radius is larger than that of the other at some scattering angles and smaller than that of the other at other scattering angles. As was discussed above, the values of $\ln(g_{total}^{(1)}(\tau))$ are influenced greatly by the relative scattered light intensity of the two kinds of particles. It is possible that the relationships among the plots of $\ln(g_{total}^{(1)}(\tau))$, $\ln(g_1^{(1)}(\tau))$ and $\ln(g_2^{(1)}(\tau))$ at different scattering angles can show the characteristic that the relative scattered light intensity

of the two kinds of particles changes as a function of scattering angle. The plots of $\ln(g_1^{(1)}(\tau))$, $\ln(g_2^{(1)}(\tau))$ and $\ln(g_{total}^{(1)}(\tau))$ produced using $\langle R_s \rangle$ and σ 120 nm, 6 nm and 200 nm, 10 nm at scattering angles 30° and 90° are used to explore the effects of the change of the relative scattered light intensity on $g_{total}^{(1)}(\tau)$. The simple situation $a = 1$ is investigated first. The results for scattering angles 30° and 90° are shown in Figs. 5a and 5b, respectively.

Figure 5 shows that the mixture of the two kinds of particles do not cause a large deviation between a line and plots of $\ln(g_{total}^{(1)}(\tau))$. Comparing to Figs. 1b and 3b, the results at a scattering angle of 90° show a different feature that the values of $\ln(g_{total}^{(1)}(\tau))$ approximate that of $\ln(g^{(1)}(\tau))$ of the kind of particles with the smaller mean static radius. It agrees with the fact that most of scattered light comes from the kind of particles with the smaller mean static radius at a scattering angle of 90° under the condition $a = 1$. Next, considering the characteristics of Fig. 5, for the mixture of the two kinds of particles a was chosen as 1, 5 and 10 at a scattering angle of 30° to increase the light intensity scattered by the particles with the smaller mean static radius and 1, 0.2 and 0.1 at a scattering angle of 90° to decrease the light intensity scattered by the particles with the smaller mean static radius. The values of $\ln(g_{total}^{(1)}(\tau))$ at scattering angles 30° and 90° are shown in Figs. 6a and 6b, respectively. Comparing to Fig. 5, Fig. 6 reveals that the values of $\ln(g_{total}^{(1)}(\tau))$ are influenced greatly by the values of the relative scattered intensity of the two kinds of particles.

For wide particle size distributions, for example $\sigma/\langle R_s \rangle = 20\%$, the plots of $\ln(g_1^{(1)}(\tau))$, $\ln(g_2^{(1)}(\tau))$ and $\ln(g_{total}^{(1)}(\tau))$ as a function of delay time τ were explored further. The results of $\ln(g_1^{(1)}(\tau))$, $\ln(g_2^{(1)}(\tau))$ and $\ln(g_{total}^{(1)}(\tau))$ produced using $\langle R_s \rangle$ and σ 120 nm, 24 nm and 200 nm, 40 nm at scattering angles 30° and 90° are shown in Figs. 7a and 7b, respectively. Figure 7 shows the same feature as Fig. 5. At a scattering angle of 30° the values of $\ln(g_{total}^{(1)}(\tau))$ almost are determined by the kind of particles with the larger mean static radius and at a scattering angle of 90° the values approximate that of $\ln(g^{(1)}(\tau))$ of the kind of particles with the smaller mean static radius. Meanwhile Fig. 7 also reveals that many reasons can cause the deviation between a line and plots of $\ln(g^{(1)}(\tau))$. Due to the deviations that cause by the mixture of the two kinds of particles or the particle size distribution and scattering angle cannot be distinguished, it is impossible to infer the size distribution of particles if other information about the particles in dispersion are unknown at a single scattering angle.

The effects that the different mixtures of the two kinds of particles in dispersion for the wide size distribution are investigated continually. As exploring the narrow particle size distribution, the values of a still were chosen as 1, 5 and 10 at a scattering angle of 30° to increase the light intensity scattered by the particles with the smaller mean static radius and 1, 0.2 and 0.1 at a scattering angle of 90° to decrease the light intensity scattered by the particles with the smaller mean static radius. The values of $\ln(g_{total}^{(1)}(\tau))$ at scattering angles 30° and 90° are shown in Figs. 8a and 8b, respectively. Comparing to Fig. 7, Fig. 8 reveals that the values of $\ln(g_{total}^{(1)}(\tau))$ are

greatly influenced by the different mixtures of the two kinds of particles in dispersion.

4 CONCLUSION

The nonexponentiality of $g_{total}^{(1)}(\tau)$ is not only determined by the particle size distribution and scattering angle but also greatly influenced by the relationship between the concentrations c , mass densities ρ and the values that the refractive index of the material expands as a function of the concentration $\left(\frac{dn}{dc}\right)_{c=0}$ of the two kinds of particles in dispersion. Under some conditions, the plots of $\ln\left(g_{total}^{(1)}(\tau)\right)$ as a function of delay time τ are consistent with a line and the mixture of the two kinds of particles do not causes the nonexponentiality of $g_{total}^{(1)}(\tau)$. At a single scattering angle, the mixture of the two kinds of particles or the size distribution of one kind of particles can makes the deviations between an exponentiality and $g^{(1)}(\tau)$, and the nonexponentiality of $g^{(1)}(\tau)$ are influenced greatly by the different mixtures of the two kinds of particles. Without other information about the particles in dispersion, it is impossible to infer the size distribution of particles accurately only based on $g^{(1)}(\tau)$ at a single scattering angle.

Fig. 1. The differences between the lines and plots of $\ln\left(g_{total}^{(1)}(\tau)\right)$, $\ln\left(g_1^{(1)}(\tau)\right)$ and $\ln\left(g_2^{(1)}(\tau)\right)$ as a function of the delay time τ . The symbols show the calculated values obtained using Eqs. 1, 4 and 5, and the lines show the linear fitting to the calculated data respectively. The results for the calculated data at scattering angles 30° and $^\circ$ are shown in a and b, respectively.

Fig. 2. The differences between the lines and plots of $\ln\left(g_{total}^{(1)}(\tau)\right)$ obtained under $a=1, 5$ and 10 as a function of the delay time τ . The symbols show the calculated values obtained using Eq. 1 and the lines show the linear fitting to the calculated data during a delay time range respectively. The results for the calculated data at scattering angles 30° and 90° are shown in a and b, respectively.

Fig. 3. The differences between the lines and plots of $\ln\left(g_{total}^{(1)}(\tau)\right)$, $\ln\left(g_1^{(1)}(\tau)\right)$ and $\ln\left(g_2^{(1)}(\tau)\right)$ as a function of the delay time τ . The symbols show the calculated values obtained using Eqs. 1, 4 and 5, and the lines show the linear fitting to the calculated data during a delay time range, respectively. The results for the calculated data at scattering angles 30° and 90° are shown in a and b, respectively

Fig. 4. The plots of $\ln\left(g_{total}^{(1)}(\tau)\right)$ obtained under $a=1, 5$ and 10 as a function of the delay time τ . The symbols show the calculated values obtained using Eq. 1, respectively. The results for the calculated data at scattering angles 30° and 90° are shown in a and b, respectively.

Fig. 5. The differences between the lines and plots of $\ln\left(g_{total}^{(1)}(\tau)\right)$, $\ln\left(g_1^{(1)}(\tau)\right)$ and $\ln\left(g_2^{(1)}(\tau)\right)$ as a function of the delay time τ . The symbols show the calculated values obtained using Eqs. 1, 4 and 5, and the lines show the linear fitting to the calculated data respectively. The results for the calculated data at scattering angles 30° and 90° are shown in a and b, respectively.

Fig. 6. The differences between the lines and plots of $\ln\left(g_{total}^{(1)}(\tau)\right)$ obtained under

a=1, 5 and 10 at a scattering angle of 30° and 1, 0.2 and 0.1 at a scattering angle of 90° as a function of the delay time τ . The symbols show the calculated values obtained using Eq. 1 and the lines show the linear fitting to the calculated data during a delay time range respectively. The results for the calculated data at scattering angles 30° and 90° are shown in a and b, respectively.

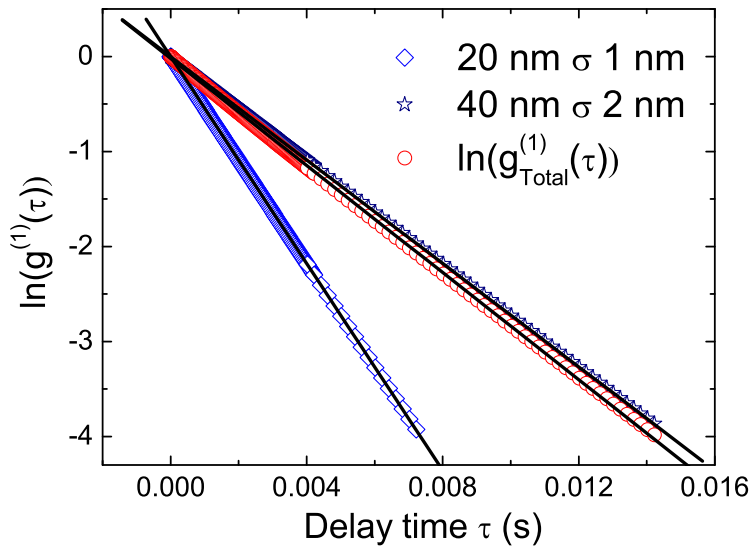
Fig. 7. The differences between the lines and plots of $\ln\left(g_{total}^{(1)}(\tau)\right)$, $\ln\left(g_1^{(1)}(\tau)\right)$ and $\ln\left(g_2^{(1)}(\tau)\right)$ as a function of the delay time τ . The symbols show the calculated values obtained using Eqs. 1, 4 and 5, and the lines show the linear fitting to the calculated data during a delay time range respectively. The results for the calculated data at scattering angles 30° and 90° are shown in a and b, respectively.

Fig. 8. The plots of $\ln\left(g_{total}^{(1)}(\tau)\right)$ obtained under a=1, 5 and 10 at a scattering angle of 30° and 1, 0.2 and 0.1 at a scattering angle of 90° as a function of the delay time τ . The symbols show the calculated values obtained using Eq. 1 respectively. The results for the calculated data at scattering angles 30° and 90° are shown in a and b, respectively.

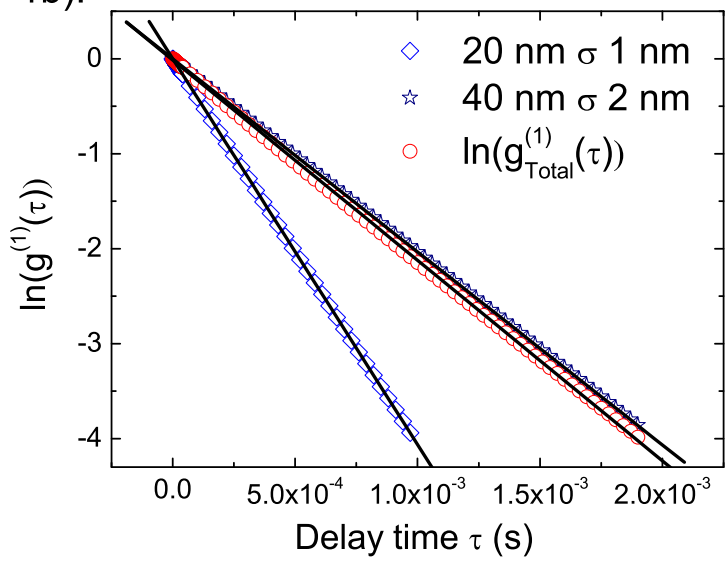
References

- [1] D. E. Koppel, J. Chem. Phys. **57**, 4814(1972).
- [2] C. B. Barger, J. Chem. Phys. **61**, 2134(1974).
- [3] J. C. Brown, P. N. Pusey and R. Dietz, J. Chem. Phys. **62**, 1136(1975).
- [4] B. J. Berne and R. Pecora, *Dynamic Light Scattering* (Robert E. Krieger Publishing Company, Malabar, Florida, 1990).
- [5] Y. Sun arxiv.org/abs/physics/0511161.
- [6] Y. Sun arxiv.org/abs/physics/0512009.
- [7] Y. Sun arxiv.org/abs/physics/0511159.
- [8] Y. Sun arxiv.org/abs/physics/0511160.

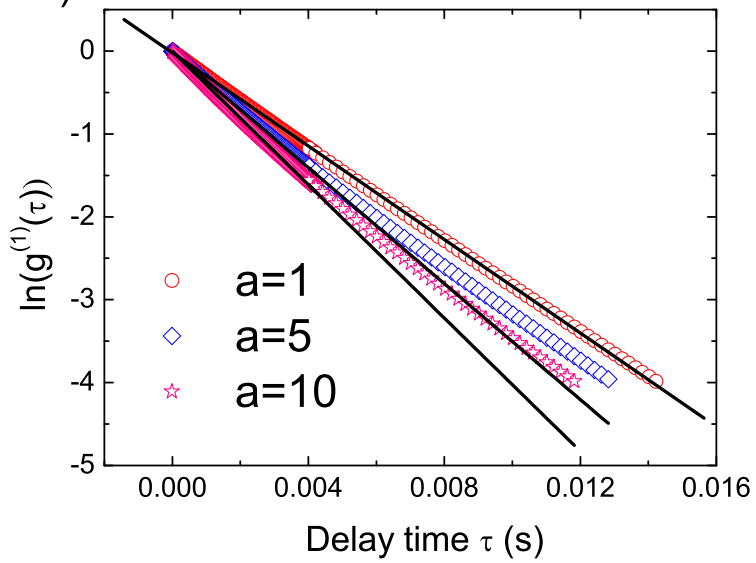
1a).



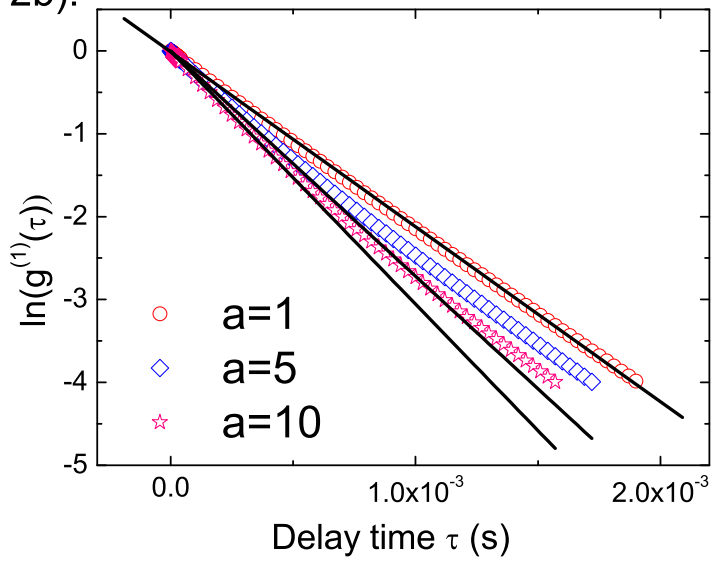
1b).



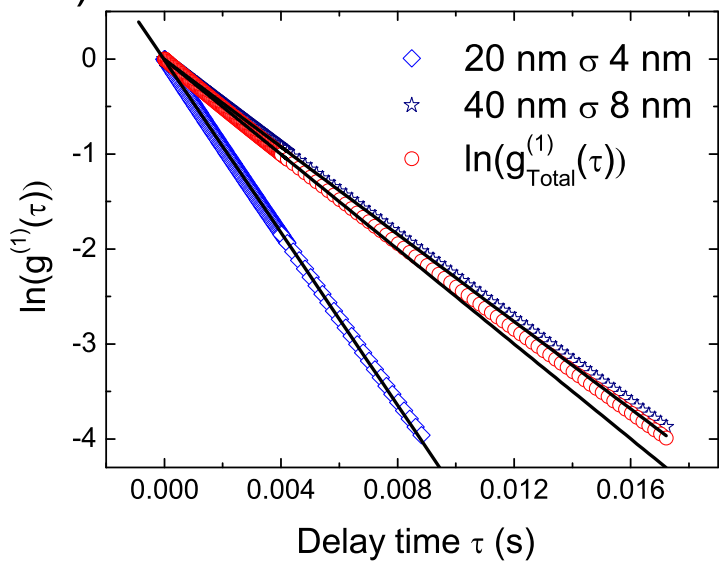
2a).



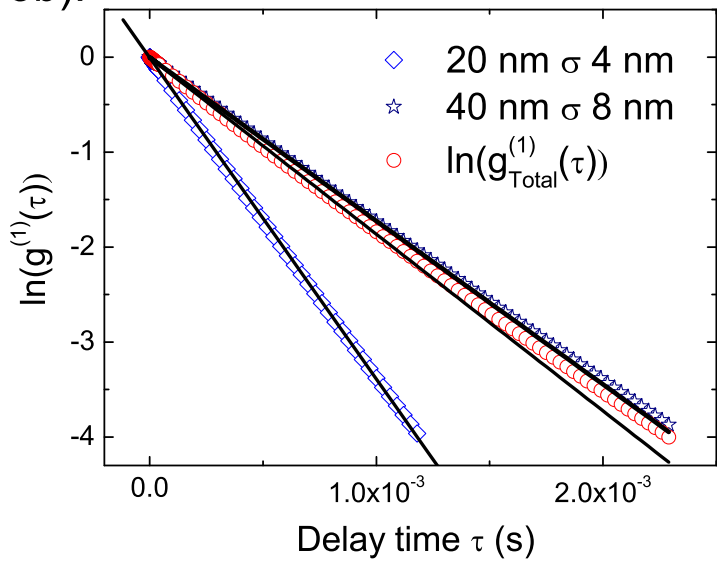
2b).



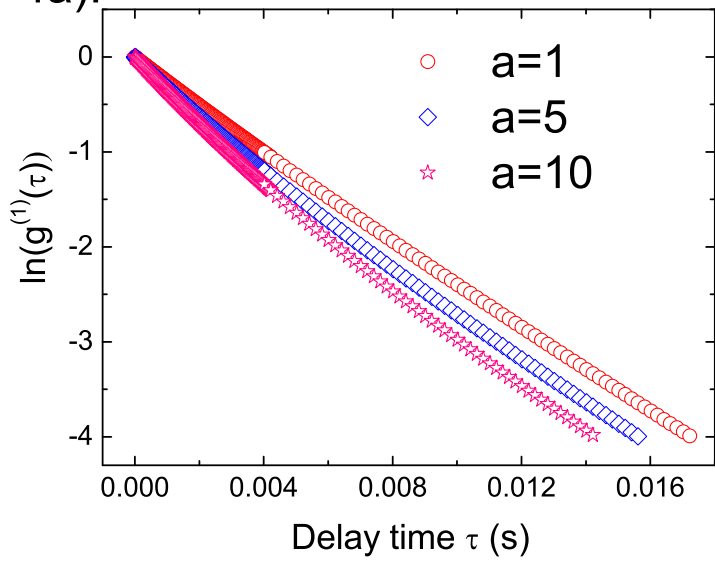
3a).



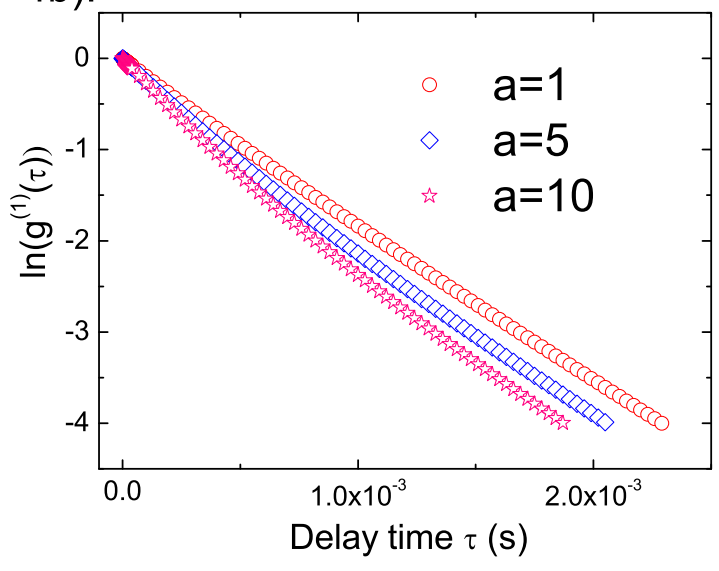
3b).

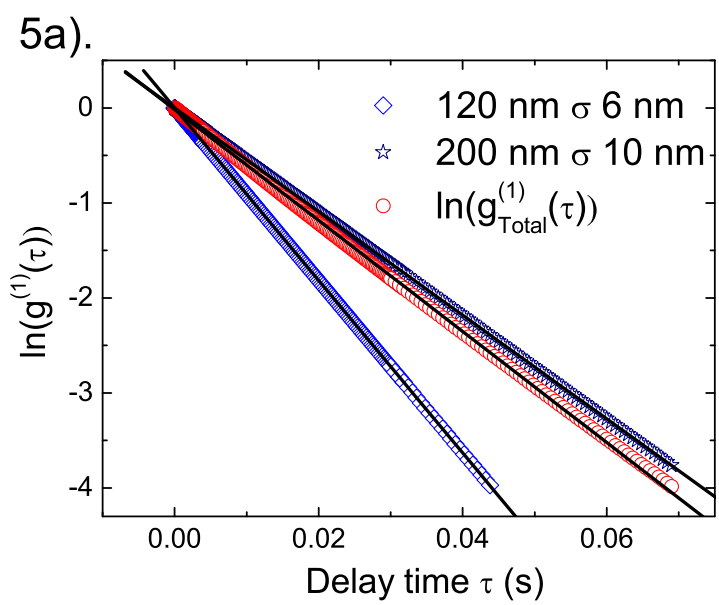


4a).

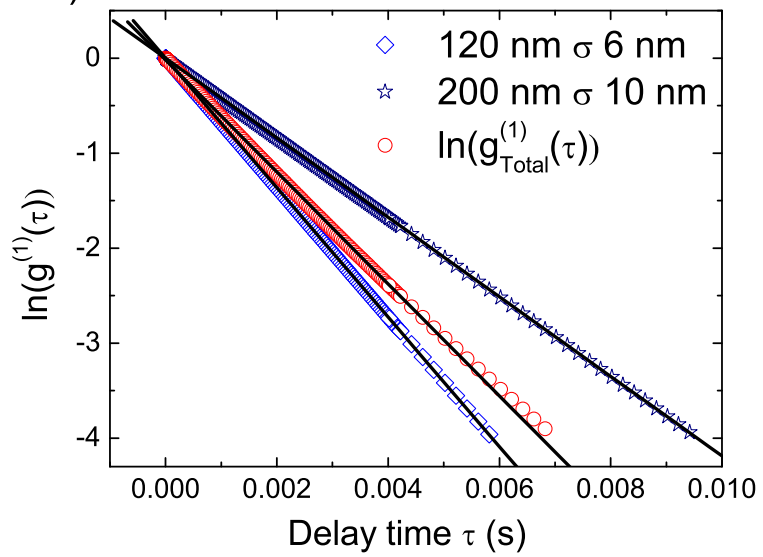


4b).

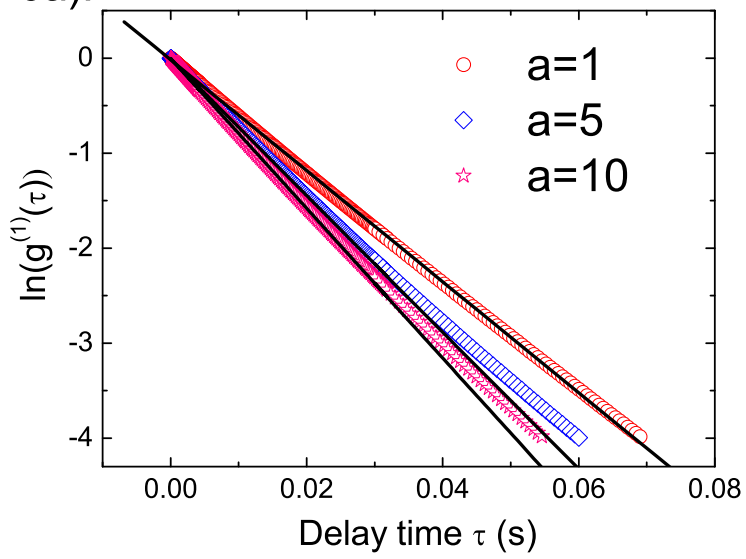




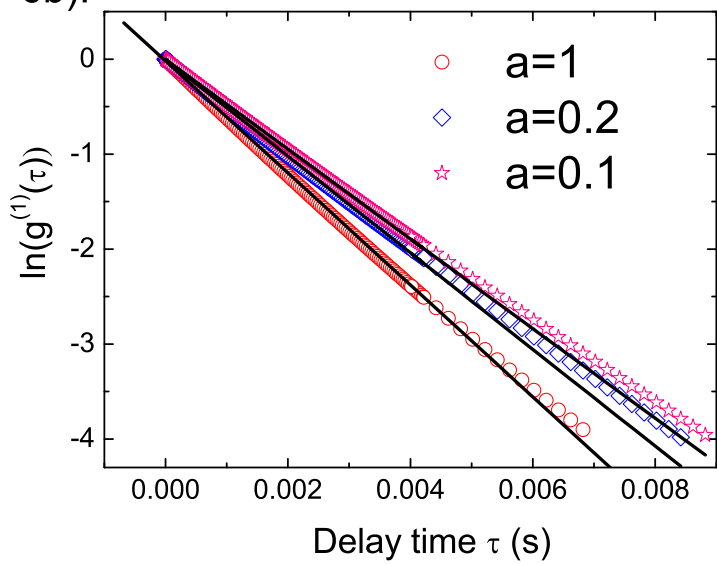
5b).



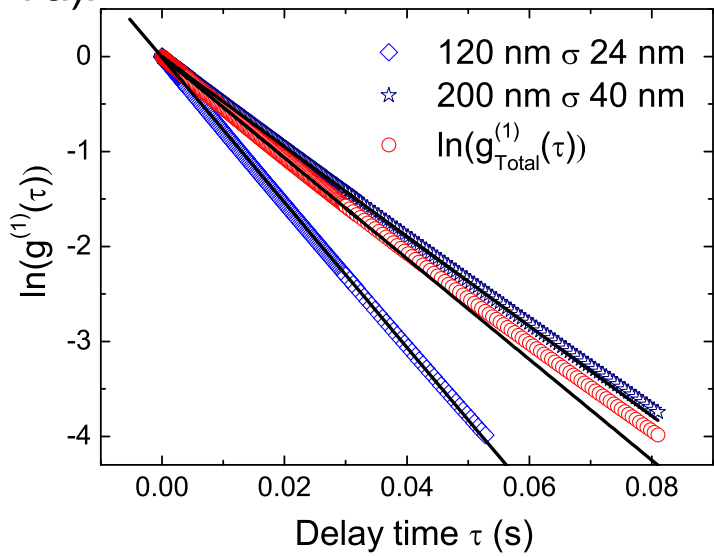
6a).



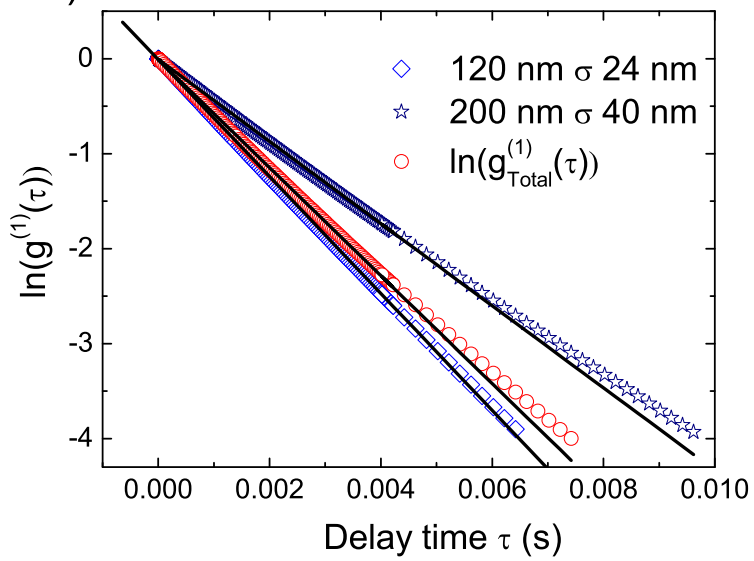
6b).



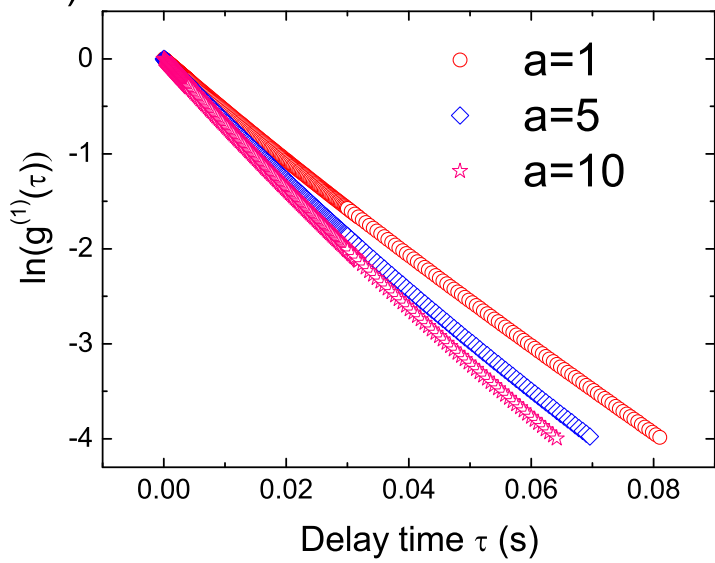
7a).



7b).



8a).



8b).

